

What happens after a fibre breaks – pull-out or resin cracking?

A. N. GENT, CHI WANG

Institute of Polymer Engineering, The University of Akron, Akron, OH 44325-0301, USA

We consider tensile fracture of a specimen consisting of a single rigid fibre embedded in a cylindrical block of a linearly-elastic resin. When the fibre breaks, two possible modes of failure can occur. A circular crack may propagate outwards into the resin, leading to fracture of the specimen. Alternatively, a cylindrical crack can propagate along the fibre–matrix interface, starting from the break in the fibre, leading to fibre pull-out. The question is: which mode of failure will occur in practice? Finite-element analysis is used here to calculate the pull-out force and the force causing growth of a circular crack outwards into the resin, for samples containing fibres of different radius. A general criterion is obtained to predict the mode of failure. Even for samples with perfect adhesion between resin and fibre, pull-out of the fibre is expected when the fibre radius is less than about one-fifth of the sample radius. For fibres of larger radius, either pull-out or resin cracking can take place, depending on the relative levels of interfacial fracture energy G_a and resin fracture energy G_c .

1. Introduction

Composite materials usually fracture either by debonding (adhesive failure) or by resin cracking (cohesive failure). Transition between cohesive and adhesive failure in a simple laminate consisting of two bonded plates has been studied by Kendall [1], both theoretically and experimentally. Corresponding transitions in fibre composites are not well understood, however. We consider here a single rigid fibre embedded along the axis of a cylindrical block of resin, assumed to be linearly-elastic (Fig. 1). Similar specimens are widely used in “fragmentation” tests of interfacial bond strength.

When the fibre breaks in tension, two possible modes of failure of the sample can take place, as shown in Fig. 1. The first is pull-out of the fibre (debonding). In this case, a cylindrical crack grows along the interface away from the fibre break. Eventually the broken fibre is pulled out of the resin block. The second is growth outwards into the resin of a circular crack initiated at the fibre break, leading eventually to rupture of the specimen. In general, two factors determine which mode of failure will actually take place. The first is the relative value of the fracture energy G_a of adhesion between fibre and resin, compared to the fracture energy G_c of the resin itself. Both G_a and G_c are independent of the geometry of the specimen. Their values can be determined from other experiments. The second factor is the effect of system geometry which determines how rapidly strain energy stored in the system is released by crack growth.

Cracking of the matrix resin is more serious than fibre pull-out, because less energy is required and the specimen breaks in a brittle way. Therefore, fibre pull-out is usually the preferred mode of failure. The crucial

question is: what criterion governs the mode of failure?

A transition from fibre pull-out to resin cracking was proposed to occur when [2]

$$\left(\frac{R_f^2}{A}\right)\left(\frac{G_a}{G_c}\right) > \frac{k}{12} \quad (1)$$

where R_f is the fibre radius, A is the cross-sectional area of the resin block and k is a constant with a value between 1 and 2. Equation 1 is based on the assumption that resin cracking becomes catastrophically unstable when the initial crack starts to grow. However, Gent and Wang [3] investigated the fracture mechanics of resin cracking both by finite-element analysis (FEA) and experimentally, and found that a circular crack will grow in a stable way until it reaches a radius of about one-half that of the resin block. Therefore, a new criterion is needed to replace Equation 1.

2. Theoretical considerations

2.1. Pull-out mode

From linear elastic fracture mechanics, the force F required to propagate a debond along the fibre–resin interface is related to the rate of increase of the sample compliance C with crack length c , as follows [4]:

$$F^2 = \frac{4\pi R_f G_a}{(dC/dc)} \quad (2)$$

Equation 2 can be stated more generally as follows:

$$F^2 = mEG_a \quad (3)$$

where E is Young’s modulus of the resin and m is a pre-factor with dimensions $[L]^3$ that can be determined by FEA, using Equation 2. For a rigid fibre

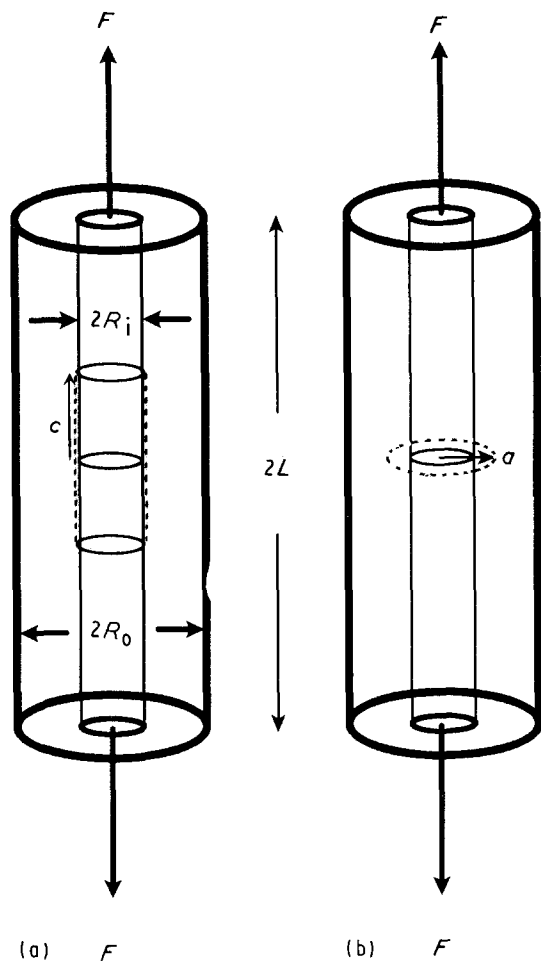


Figure 1 Sketch of the model: (a) pull-out mode, (b) resin cracking mode.

embedded in a long cylindrical block of an elastic cylinder, a simple energy balance calculation yields a value for m of $4\pi^2(R_0^2 - R_1^2) R_1$ when the interfacial crack is relatively long, where R_1 is the fibre radius and R_0 is the radius of the elastic block in which the fibre is embedded [2].

Pull-out of a broken fibre is shown schematically in Fig. 1a. Theoretically, two cylindrical cracks can grow apart simultaneously along the interface, as shown, leading to pull-out of both parts of the broken fibre. However, only one crack is observed in practice. The analysis for two cracks is simpler, using symmetry conditions, and is adopted here for that reason. In some trial calculations the results were found to be indistinguishable from the one-crack case. (When the cracks are relatively long the results are clearly identical, because the volume of matrix subjected to simple extension becomes twice as large as for a single crack, while the energy used in debonding is also twice as large.)

2.2. Resin cracking mode

The force F required to make a circular crack grow is related to the rate of increase of compliance C with crack radius a , as follows [4]:

$$F^2 = \frac{4\pi a G_c}{(dC/da)} = 4\pi a (R_0 - R_1) \frac{E G_c}{f} \quad (4)$$

where G_c is the fracture energy of the resin and f is given by

$$f = \frac{d(CE)}{d[(a - R_1)/(R_0 - R_1)]} \quad (5)$$

The quantity $(a - R_1)/(R_0 - R_1)$ is a reduced crack radius.

In general, catastrophic fracture takes place when the crack is half-way to the edge [3], i.e. when

$$a_c = \frac{R_1 + R_0}{2} \quad (6)$$

The fracture force F_b at this critical radius can be determined by FEA calculation, using Equations 4 and 5.

3. Simulation details

FEA calculations were carried out using the ADINA code [5]. Only one-half of the specimen was modelled because of the symmetry of the system. The finite-element grid is shown schematically in Fig. 2. Axisymmetric quadrilateral eight-noded elements, with nine integration points, were used—fifteen in the radial direction and thirty in the axial direction, for a total of 450. Both the central fibre and the matrix resin were assumed to be incompressible and linearly-elastic. The

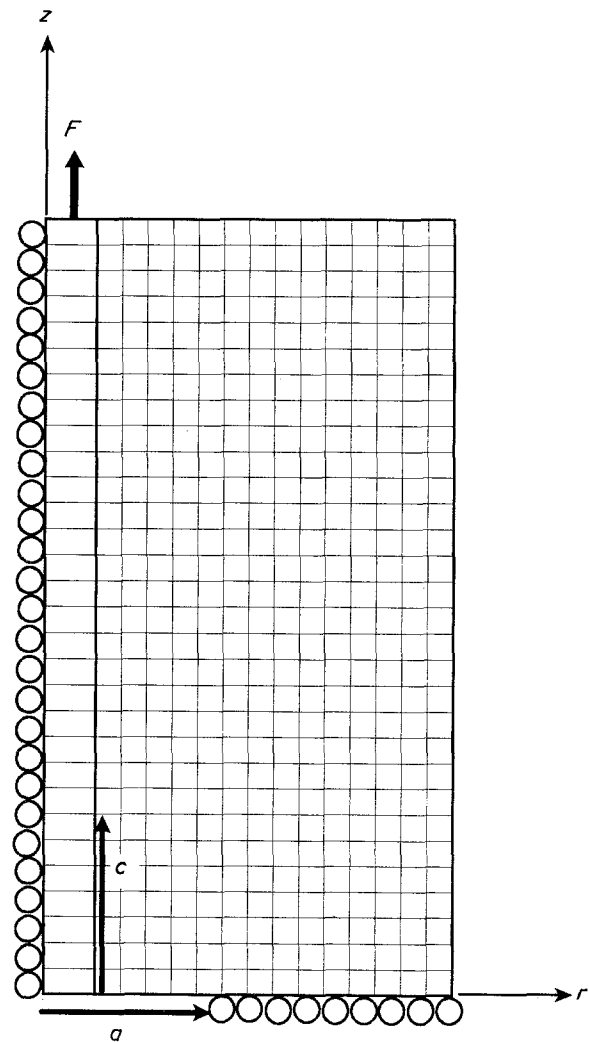


Figure 2 Finite-element grid (schematic).

fibre was made nine orders of magnitude stiffer than the matrix, to be effectively rigid. Various values were assigned to the fibre radius R_i and sample radius R_o . To avoid end effects, the sample length was taken to be much longer than R_o , at least $15 \times [3]$.

For interfacial cracking, contact elements were employed at the fibre-resin interface with zero friction. Compliances were calculated for different crack sizes and hence values of dC/dc and m , from Equations 2 and 3. For lateral cracking, when a circular crack grows outwards into the resin, the method of determining dC/da , and hence f , using Equation 5, is similar [3].

Values of the force F required to propagate the crack, either in debonding or in resin cracking, can be determined by means of Equations 3 and 4, in terms of the corresponding fracture energy, G_a or G_c . When the bonding is perfect, G_a is assumed to be equal to G_c .

3.1. Mixed-mode fracture

When the fibre breaks it creates a circular crack of the same radius, which may then grow outwards into the resin. Subsequently, as the force required to propagate the crack increases, a second crack may start to grow along the fibre, leading eventually to pull-out. Thus, a two-stage fracture process is possible, shown schematically in Fig. 3. This possibility was investigated using a sample with fibre radius R_i of 0.15 mm and

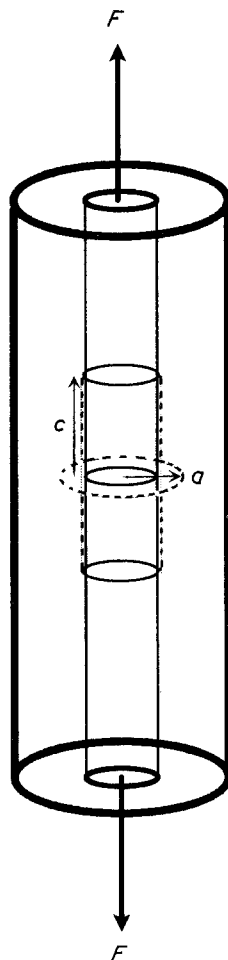


Figure 3 Sketch of two-stage fracture.

sample radius R_o of 3 mm. Debonding failures were studied for three sizes of the lateral crack, with $a/R_i = 1.2, 2$ and 5 . The tendency for pull-out to occur after some resin cracking has taken place is discussed in the light of these results.

4. Results and discussion

4.1. Mechanics of pull-out

A typical relationship between calculated compliance and crack length c is shown in Fig. 4 for samples with $R_i/R_o = 0.145$. All the other samples studied showed the same trend. The compliance increased dramatically for small debonds, up to a length of about $3R_i$. Then a linear relation was found to hold between compliance and crack size until the crack length became comparable to the sample length.

The dramatic increase in compliance at small debonds suggests that only a small force is necessary to initiate crack growth (Equation 2). After the compliance becomes linearly dependent on crack length, a constant pull-out force is expected. From the slopes of the linear portions of relations obtained in this way, values of m were calculated using Equations 2 and 3. A comparison of calculated values with those obtained from a simple energy balance, $4\pi^2(R_o^2 - R_i^2) R_i$ [2], is given in Table I. Good agreement is obtained. Moreover, they agree with values obtained experimentally when frictional effects were minimized [6]. Thus, FEA results for long cracks are in good agreement with results from a simple energy balance calculation.

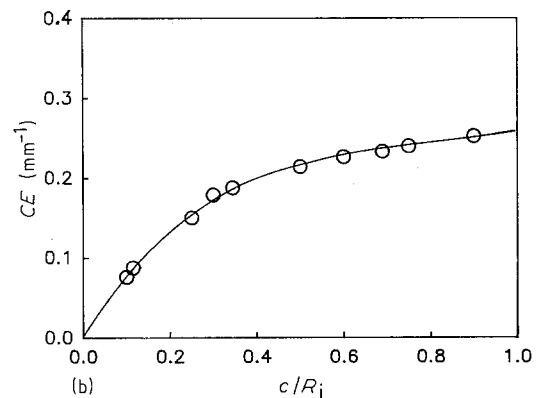
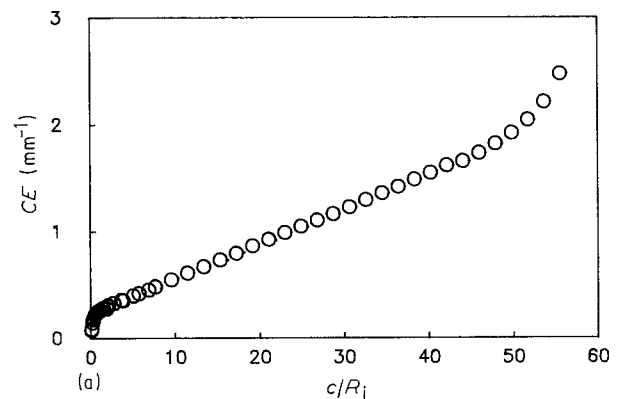


Figure 4 (a) Typical relation between CE and length c of a debond crack, where C is sample compliance and E is Young's modulus of the resin; $R_i = 0.435$ mm, $R_o = 3.0$ mm. (b) Expanded view of the initial region of (a).

4.2. Mechanics of resin cracking

A typical relationship between calculated compliance and crack radius is shown in Fig. 5 for a sample with $R_i/R_o = 0.145$. The trend is similar to that found for interfacial cracks. Again, the compliance increased dramatically for small cracks and then followed an approximately linear dependence for values of dimensionless crack radius $(a - R_i)/(R_o - R_i)$ in the range of 0.15 to 0.6. This feature was found to hold for all of the samples studied. Thus, dC/da is largely independent of crack size over a substantial range. This means that the force required to propagate the crack is proportional to $a^{1/2}$ (Equation 4) and thus increases with crack radius.

Calculated relations between compliance and crack radius are shown in Figs 6 and 7 for different values of R_i and R_o . Values of f were determined from the slopes

TABLE I Comparison of m values (Equation 3) for long cracks obtained from FEA and from theory, $m = 4\pi^2(R_o^2 - R_i^2)R_i$, for samples with different fibre radius R_i

R_i (mm)	R_o (mm)	m (mm) ³ from theory	m (mm) ³ by FEA	Relative error (%)
0.15 ^a	3.0	53	53	0.0
0.43 ₅ ^a	3.0	151	145	-4.2
1.00 ^b	3.0	316	318	+0.7
1.50 ^b	3.0	400	401	+0.3

^a $L = 25$ mm.

^b $L = 50$ mm.

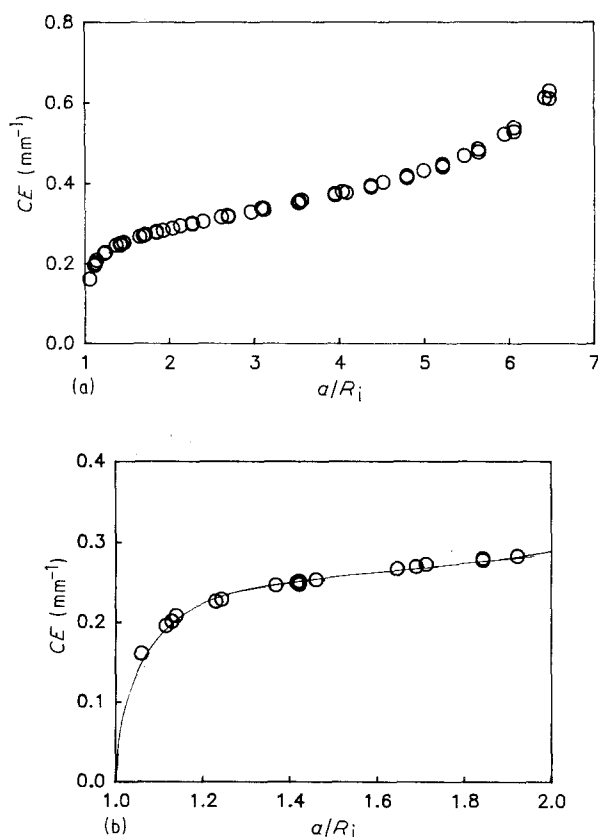


Figure 5 (a) Typical relation between CE and crack radius a for resin cracking; $R_i = 0.435$ mm, $R_o = 3.0$ mm. (b) Expanded view of the initial region of (a).

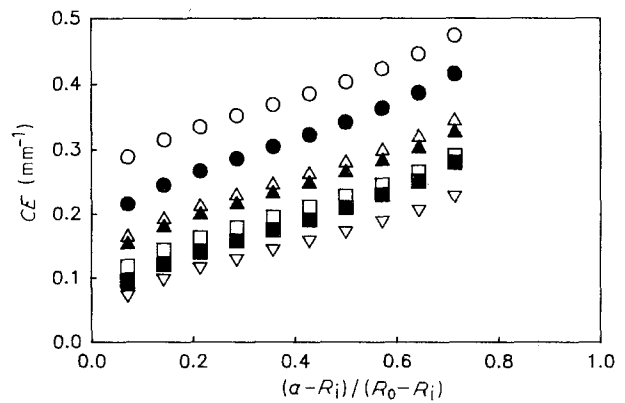


Figure 6 Calculated relation between compliance and crack radius for different values of R_i ($R_o = 3.0$ mm); R_i (mm) = (O) 0.3, (●) 0.6, (Δ) 0.9, (▲) 1.0, (□) 1.5, (■) 2.0, (▽) 2.4.

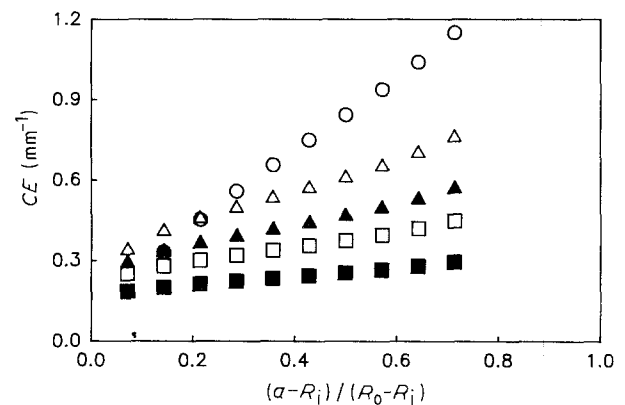


Figure 7 Calculated relation between compliance and crack radius for different R_o ($R_i = 0.435$ mm); R_o (mm) = (O) 0.54, (Δ) 1.45, (▲) 2.18, (□) 3.00, (■) 5.60.

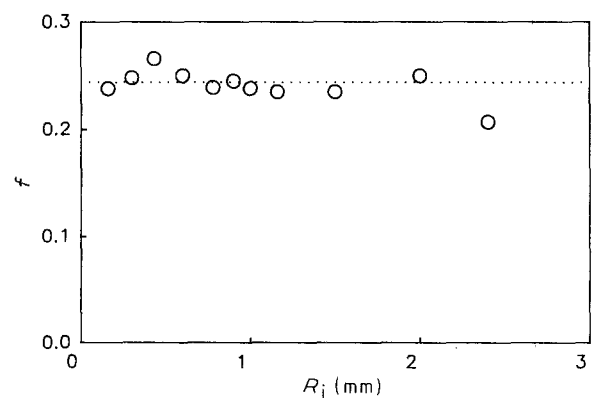


Figure 8 Variation of f with R_i ($R_o = 3.0$ mm).

and are plotted in Figs 8 and 9. They are seen to be approximately independent of fibre radius R_i and approximately proportional to $1/R_o$, where R_o is the sample radius. By linear regression analysis, the function f is found to take the form

$$f = 0.75/R_o \quad (7)$$

Thus, the force that will cause catastrophic failure is obtained by substituting Equations 6 and 7 into Equation 4:

$$F_b^2 = \frac{8\pi}{3}(R_o^2 - R_i^2) R_o EG_c \quad (8)$$

Equation 8 is in good accord with experimental measurements of fracture force, as shown in Table II. We conclude that the fracture force depends strongly on sample radius, but not much on fibre radius.

By comparing the fracture force given by Equation 8 with the corresponding force for fibre pull-out given by Equation 3, a transition from pull-out to resin cracking is expected to occur when

$$\frac{R_i}{R_o} \geq \frac{2}{3\pi} \left(\frac{G_c}{G_a} \right) \quad (9)$$

Thus, pull-out is expected to take place if R_i/R_o is less than 0.21, even when the value of the interfacial strength G_a is as high as the strength G_c of the matrix. And, of course, pull-out will take place when the ratio R_i/R_o is greater than 0.21 if the level of adhesion is lower. In other words, lateral cracking will occur for fibres of relatively large radius if the adhesion is strong, but pull-out is inevitable for fibres of relatively small radius, even when the bond is as strong as possible.

4.3. Pull-out or resin cracking

Generally speaking, the effect of R_i on the fracture force for lateral cracking is insignificant when the ratio R_i/R_o is small. All samples have a similar breaking force (Equation 8). On the other hand, the pull-out force increases with fibre radius, as shown in Equation 2. Thus, a transition from pull-out to lateral cracking would be expected as the fibre radius is increased. Assuming that the values of G_a and G_c are the same, the forces required to propagate a debond and a circular crack can be calculated from Equations 2 and 4, and compared. The force needed to initiate a debond is estimated by extrapolating the pull-out force back to a crack length of zero. In the resin cracking case, the force to initiate a circular crack is estimated by extrapolating the force back to a crack radius equal to the fibre radius. A comparison has been made in this way between initial and final values of a reduced pull-out force $F/(EG_a)^{1/2}$ and a corresponding reduced resin-cracking force $F/(EG_c)^{1/2}$, for different fibre radii, as shown in Figs 10–12. They are given in Table III.

The force to initiate a debond is larger than that to initiate a circular crack at the fibre end in all cases, if the strength of the interface is as high as the strength of the matrix, i.e. $G_a = G_c$. Therefore, a circular crack starts to grow first when a tensile load is applied to the fibre. This circular crack may continue to grow if the ratio R_i/R_o is relatively large, greater than about 0.21;

TABLE II Catastrophic failure force $F' = F_b/(EG_c)^{1/2}$ for resin cracking

R_i (mm)	R_o (mm)	F' (mm ^{3/2})	
		Experiment [3]	Equation 8
0.43 _s	3.0	13.2	14.8
0.78	3.0	13.6	14.6
1.00	3.0	14.0	14.2
1.16	3.0	13.2	13.8
0.43 _s	5.6	40.2	38.3

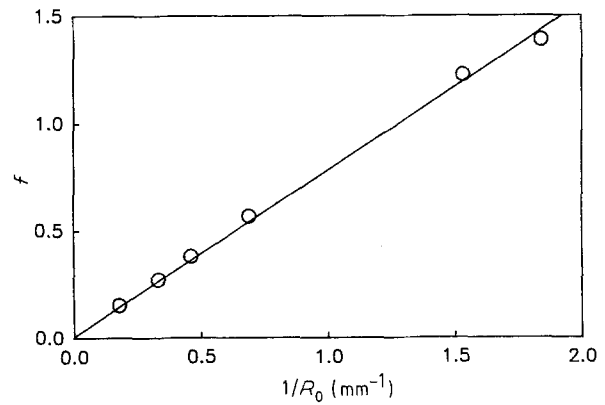


Figure 9 Variation of f with R_o ($R_i = 0.435$ mm).

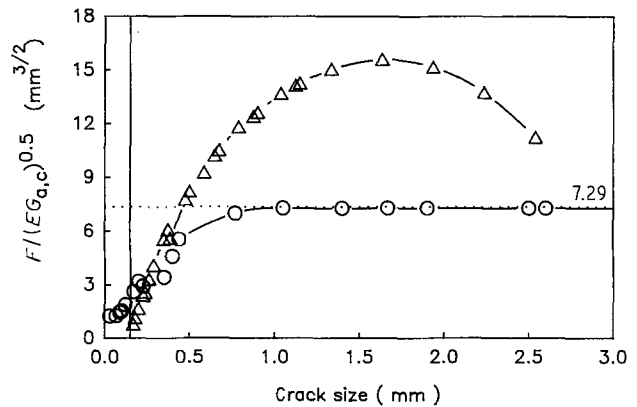


Figure 10 Reduced forces for (○) pull-out $F_p/(EG_a)^{1/2}$ and (△) resin cracking $F_c/(EG_c)^{1/2}$ for samples with $R_i = 0.15$ mm, $R_o = 3.0$ mm.

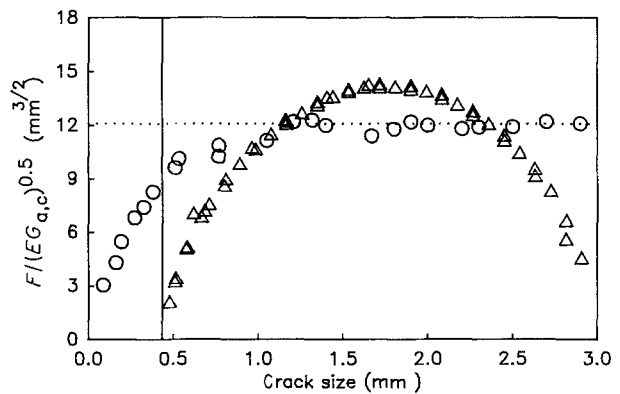


Figure 11 Reduced forces for (○) pull-out $F_p/(EG_a)^{1/2}$ and (△) resin cracking $F_c/(EG_c)^{1/2}$ for samples with $R_i = 0.435$ mm, $R_o = 3.0$ mm.

but if R_i/R_o is smaller than 0.21, it might stop growing—pull-out will take place instead. This is because the final pull-out force is smaller than the maximum force at which catastrophic cracking of the matrix occurs. Therefore, samples with small-radius fibres are expected to fail by pull-out, but with a small circular crack at the fibre ends. An example is discussed below.

4.3.1. Fibres of relatively small radius

For a sample with $R_i = 0.15$ mm and $R_o = 3.0$ mm, a smaller force is required to initiate cracking of the

TABLE III Computed forces for initiation F_i and final failure F_b in pull-out or resin cracking^a

R_i (mm)	Pull-out		Resin cracking	
	$F_i/(EG_a)^{1/2}$ (mm ^{3/2})	$F_b/(EG_a)^{1/2}$ (mm ^{3/2})	$F_i/(EG_c)^{1/2}$ (mm ^{3/2})	$F_b/(EG_c)^{1/2}$ (mm ^{3/2})
0.15	1.33	7.29	0.25	14.83
0.43 _s	2.43	12.05	0.67	14.08
1.00	4.49	17.8 ^b	1.38	14.45
1.50	6.87	20.0 ^b	2.80	13.33

^a $R_o = 3.0$ mm, $L = 25$ mm.

^b $L = 50$ mm.

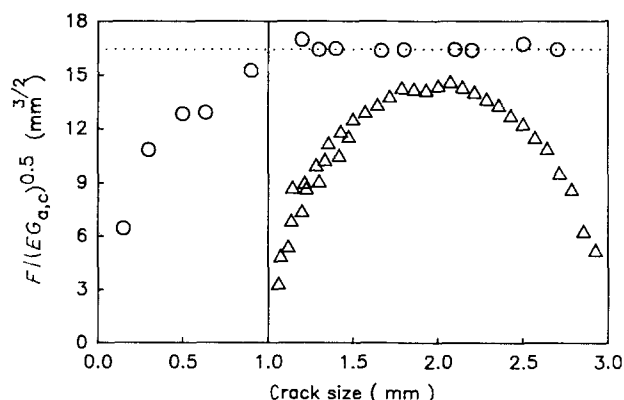


Figure 12 Reduced forces for (○) pull-out $F_p/(EG_a)^{1/2}$ and (△) resin cracking $E_c/(EG_c)^{1/2}$ for samples with $R_i = 1.0$ mm, $R_o = 3.0$ mm.

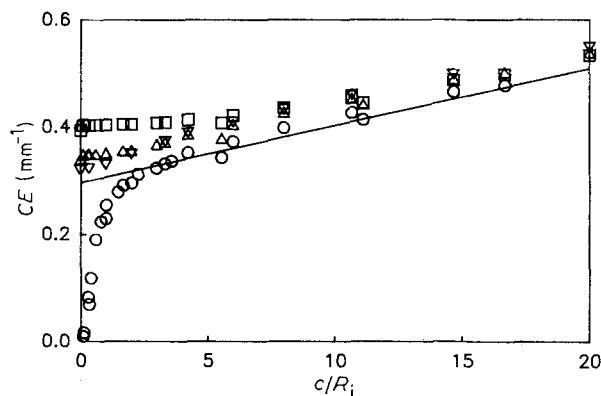


Figure 13 Variation of sample compliance C with length c of interfacial crack for samples with circular cracks of different radius at the fibre end: (○) 0.15 mm, (▽) 0.18 mm, (△) 0.30 mm, (□) 0.75 mm.

matrix rather than pull-out of the fibre (Fig. 10). Thus, after a fibre breaks it is more likely that a circular crack will grow outwards into the matrix than that a cylindrical crack will propagate along the fibre–matrix interface. However, the final fracture force to cause the sample to fail by resin cracking is about twice as large as that for pull-out. The two force curves cross at a lateral crack radius of about 0.3 mm (Fig. 10). Thus, the lateral crack will tend to stop growing at a radius of about 0.3 mm, and pull-out will occur instead.

Values of compliance for a two-stage fracture of this type are shown in Fig. 13. If no growth of a lateral crack takes place after the fibre breaks, i.e. $a = 0.15$ mm, the compliance increases dramatically with length c of a debond. On the other hand, when the radius a of the lateral crack is 0.18 mm, the compliance increases linearly with the length of a debond, even in the small debond region. The calculated forces to initiate and to propagate the debond are then about the same, a little higher than the value to propagate a debond with no lateral crack.

When the lateral crack radius a is 0.75 mm, the change of compliance as a debond grows is rather small for small debonds, up to about 0.75 mm. This suggests that it is difficult to initiate a debond when a relatively large lateral crack has formed at the fibre end. For longer debonds, when c/R_i is greater than about 10, a linear relation is again obtained between compliance and debond length, corresponding to a constant debonding force.

To summarize, the energy release rate for a debond crack is reduced by the presence of a circular crack at

the fibre ends. Therefore, a higher force is required to initiate a debond. On the other hand, the energy release rate for lateral cracking is decreased significantly as the debond length increases [7]. Thus, if some debonding takes place, a larger stress will be required to initiate resin cracking.

The most likely mode of fracture for samples with $R_i = 0.15$ mm and $R_o = 3.0$ mm is that a circular crack will grow outwards, from its initial radius of 0.15 mm up to a radius of 0.47 mm. Simultaneously, the applied force will increase up to a value high enough to initiate a debond even in the presence of the circular crack. Since no further increase in load is required to propagate the debond after it initiates, pull-out will then occur rather than resin cracking. Thus, the sample is expected to fail eventually by pull-out, but with a circular crack of about 0.47 mm radius at the fibre end.

4.3.2. Fibres of larger radius

For a sample with $R_i = 0.435$ mm and $R_o = 3.0$ mm, a lateral crack will again be initiated at a force smaller than the force to initiate debonding. Although the force for crack propagation increases with increasing crack radius, the maximum force for catastrophic rupture is only slightly higher than the final pull-out force, as shown in Fig. 11. Therefore, pull-out seems to be rather unlikely. Fracture will probably take place by continuous growth of a circular crack in the resin until catastrophic failure occurs.

For samples with $R_i = 1.0$ mm and $R_o = 3.0$ mm, there is no crossover between pull-out force and resin-cracking force over the whole range of crack radius (Fig. 12). The force to initiate pull-out is always higher. This implies that resin cracking is inevitable – there will be no tendency for fibre pull-out to occur.

5. Conclusions

After a fibre breaks, either pull-out or resin cracking can take place. Because of the high stress concentration at the break, a relatively small force is needed to initiate either mode of failure. Generally, a small resin crack will form first. Then, for small-radius fibres a new crack will propagate along the fibre interface at a pull-out force which reaches a constant value (in the absence of friction), given by Equation 3. On the other hand, for larger fibres a circular crack will propagate outwards into the resin under a force which increases until the sample fractures, at a crack radius of about $(R_o + R_i)/2$ and at a breaking force given by Equation 8. Which mode of failure occurs depends upon the relative magnitude of the forces required. However, it should be noted that friction at the fibre–resin interface will cause the pull-out force to increase to larger values than those considered here, making resin

cracking more probable in such cases [6]. It has often been observed in fragmentation tests that complicated fractures take place after the fibre breaks, including debonding and resin cracking. These effects can be attributed in part to the relative strengths of adhesive and cohesive failures and in part to geometrical factors, as discussed above.

References

1. K. KENDALL, *Proc. Roy. Soc. (London)*, **A344** 287 (1975).
2. A. N. GENT, G. S. FIELDING-RUSSELL, D. I. LIVINGSTON and D. W. NICHOLSON, *J. Mater. Sci.* **16** 949 (1981).
3. A. N. GENT and C. WANG, *ibid.* **27** 2539 (1992).
4. J. G. WILLIAMS, "Fracture Mechanics of Polymers" (Wiley, New York, 1984) p. 30.
5. K. J. BATHE, "ADINA: A Finite Element Program for Automatic Dynamic Incremental Non-Linear Analysis", Report No. 82448-1 (Massachusetts Institute of Technology, Cambridge, Massachusetts, 1977).
6. A. N. GENT and G. L. LIU, *J. Mater. Sci.* **26** (1991) 2467.
7. U. MBANEFO and R. A. WESTMANN, *Trans. ASME* **57** (1990) 654.

*Received 17 June
and accepted 6 July 1992*